

A multi-proxy reconstruction of tropical cyclone variability during the past 800 years from Robinson Lake, Nova Scotia, Canada

F. Oliva^{a,*}, M.C. Peros^b, A.E. Viau^a, E.G. Reinhardt^c, F.C. Nixon^{d,1}, A. Morin^a

^a Laboratory for Paleoclimatology and Climatology, University of Ottawa, Ottawa, Ontario, Canada

^b Department of Environment and Geography, Bishop's University, Sherbrooke, Québec, Canada

^c School of Geography & Earth Sciences, McMaster University, Hamilton, Ontario, Canada

^d Geoscience and Mines Branch, Department of Natural Resources, Government of Nova Scotia, Halifax, Nova Scotia, Canada

ARTICLE INFO

Editor: Michele Rebesco

Keywords:

North Atlantic
Paleotempestology
Tropical cyclones
X-ray fluorescence
Grain size analysis

ABSTRACT

This study presents a multi-proxy reconstruction of tropical cyclone (TC) activity for the past 800 years from Robinson Lake, located on the north Atlantic seaboard of Nova Scotia, Canada. Two sediment cores were extracted from Robinson Lake and were dated by ²¹⁰Pb and ¹⁴C methods, and analyzed for organic matter content, sediment grain size, and a range of elements and elemental ratios determined by XRF core scanning. A distinct sand layer in the most recent sediments is attributed to Hurricane Juan, which struck the coast of Nova Scotia on September 29, 2003. Our study shows that peaks in grain size farther down-core are generally correlated with abrupt increases in Br and Br/Ti. XRF-derived Br measurements are an indicator of marine organic carbon (MOC), and the increases in Br likely reflect incursions of marine water and nutrients into the lake as a result of storm surges. The results show that the period from ~1475 to 1670 CE contains at least 3–4 storm beds, and are interpreted as the most active TC period within the last ~800 years for this region. Our results are consistent with recent research from Salt Pond, Massachusetts (Donnelly et al. 2015), which provides evidence for heightened TC activity during the same period as our study at Robinson Lake. Our study represents one of the highest latitude paleotempestological studies from the North Atlantic basin which will help the testing of hypotheses concerning long-term changes in North Atlantic TC activity under future climate change scenarios.

1. Introduction

North Atlantic tropical cyclones (TCs), also known as hurricanes, and their associated winds and storm surges, have resulted in major impacts on coastal ecosystems and human infrastructure (Emanuel, 2003). Continuous and reliable instrumental data, which extends back at most ~70 years, and historical data, which can go back hundreds of years but is often incomplete (Liu, 2004), do not provide the long-term perspectives necessary for reconstructing past and modelling future trends in TC activity (Toomey et al., 2013). For example, Mann et al. (2009) suggested that there may have been enhanced TC activity during the Medieval Climate Anomaly (MCA, 900–1200 CE) in the North Atlantic, which could be an analogue for future warming expected for this region (Rhein et al., 2013), but long-term paleotempestological reconstructions to test this idea, especially from mid-latitude regions, are rare (but see Donnelly et al., 2001, 2004, 2015).

In this study, we present an 800-year record of TC activity from a

small lake on the Atlantic coast of central Nova Scotia, Canada. The Canadian Maritimes have been the focus of limited paleotempestological research (e.g. Schafer and Medioli, 2009), despite being affected by TC activity (Hurricane Juan, for example, was responsible for billions of dollars of damage when it struck the coast of Nova Scotia in September 2003) (McTaggart-Cowan et al., 2006). Although this region has been extensively studied for sea-level and other paleoclimatic indicators (e.g., Chagué-Goff et al., 2001; Gehrels et al., 2005; Scott et al., 1995), this study adds important new insight to the north-western limit of North Atlantic TC tracks. In this way, this study from Nova Scotia permits us to better explore how large-scale climatic events, such as the El Niño–Southern Oscillation (ENSO) (Donnelly and Woodruff, 2007), and the position of the Bermuda High (Liu and Fearn, 2000), influence TC activity over multiple timescales (Toomey et al., 2013). Marine inundation of coastal lakes or lagoons in this region is not limited to TCs but can also be caused by mid-latitude winter oceanic storms (i.e. nor'easters) (e.g., Donnelly et al., 2004) and to a lesser extent, tsunamis

* Corresponding author at: 60 University Prvt. Simard Hall., Dept. Of Geography, University of Ottawa, Ottawa, Ontario K1N6N5, Canada.
E-mail address: foliva@uottawa.ca (F. Oliva).

¹ New address: Department of Geography, Norwegian University of Science and Technology, Trondheim, Norway.

(e.g., Moore et al., 2007; Tuttle et al., 2004). Differentiating between the three types of events can be challenging (Toomey et al., 2013), and we address this through an analysis of the modern (i.e., 20th and early 21st century) sediments at the site and compare these to instrumental data of past storm surges from Halifax (located approximately 20 km to the west of Robinson Lake).

Several field techniques and laboratory analyses have been used in paleotempestological research (Wallace et al., 2014; Oliva et al., 2017). The most widely used approach includes established laboratory analyses such as sediment grain-size and organic matter content, and analyses of micropaleontological indicators sampled from sediment cores extracted from coastal settings (e.g. Liu and Fearn, 2000; Donnelly et al., 2004; Scott et al., 2003; McCloskey and Liu, 2012; van Hengstum et al., 2014). Other more recent approaches include: 1) multi-proxy analyses of deep-sea cores (Toomey et al., 2013); 2) X-ray fluorescence (XRF) and geochemical analyses of sediments (Woodruff et al., 2008; Brandon et al., 2014); and 3), tree cellulose and speleothem isotopic analyses (Miller et al., 2006; Frappier et al., 2007). Over the last two decades, X-ray fluorescence (XRF) core scanners have become increasingly utilized in paleoenvironmental research. Originally used to identify the elemental composition of marine sediments, XRF core scanning is increasingly used on lake and terrestrial deposits (Rothwell and Croudace, 2015; Kylander et al., 2011a; Croudace et al., 2006). Elemental proxy data can provide high-resolution time series useful for the study of variations in chemistry, mineralogy, and biological primary productivity, which may ultimately be linked to climatic and environmental change (eg. Itambi et al., 2009; Ziegler et al., 2008; Croudace et al., 2006).

A relatively large body of paleotempestological research has now been conducted along the north shore of the Gulf of Mexico and the eastern seaboard of the United States (e.g. Wallace et al., 2014; Oliva et al., 2017), but little is known about past TC activity north of New England. In this study we use a multiproxy approach (sediment grain-size, loss on ignition, and XRF core scanning) to study a small lake (Robinson Lake) on the western seaward edge of Chezzetcook Inlet for the purpose of reconstructing past TC activity for this region. Conducting research in Nova Scotia contributes to filling important geographical gaps in the coverage of paleotempestological data and helps us understand past TC dynamics at the northern margin of the Atlantic hurricane zone (see Oliva et al., 2017). This is important because marginal areas (such as the Canadian Maritimes) may provide records which are more sensitive to changes in TC activity as a result of climate change, and hence help us better understand how TC activity may vary in the future.

2. Study site

In selecting our field site, it was of primary importance to locate a coastal lake known to be affected by TCs. Robinson Lake was hit directly by Hurricane Juan on September 29th, 2003 (NOAA, 2018) and local residents confirmed that the barrier was breached during that event (personal communication, John Donahue, 2014 – Local resident and Nova Scotia Department of Natural Resources Scientist). The second criterion was that, under normal conditions, the lake water is fresh or low-salinity (as opposed to marine). Robinson Lake was tested in several locations and found to have an average salinity of < 5‰, classifying it as oligohaline. Next, the study site needed to be non-tidal, confirming its separation from the marine system. Finally, a stable barrier, elevated high enough above mean sea level, was required to ensure that the lake was not getting regularly breached during normal high tides or storms.

Robinson Lake is located at sea-level at 44°39.114'N 63°16.631'W, on the western margin of the mouth of Chezzetcook Inlet (Fig. 1a). Chezzetcook Inlet has been previously studied by groups led by Dr. David Scott and the late Dr. Franco Mediolli at Dalhousie University for micropaleontology (e.g. Scott and Mediolli, 1980), sea-level change (e.g.

Gehrels et al., 2005), as well as salt marsh evolution (Chagué-Goff et al., 2001). Chezzetcook Inlet is a shallow estuarine environment with extensive networks of intertidal mudflats and salt marshes (Scott, 1977). The inlet formed ~4000 yr BP as a result of relative sea-level rise due mainly to the ongoing glacioisostatic adjustment of Nova Scotia (i.e., crustal subsidence; Scott et al., 1995) along with a forebulge going through the area ~1700 yr BP (Laidler and Scott, 1996). European settlement began around 200 years ago in this area; that, and modern infrastructure development in the recent past, have contributed to changes in sedimentation rates at the head of the inlet (Scott, 1980). Relative sea level (RSL) studies from the area indicate that RSL at Chezzetcook Inlet was ~1 m lower 1000 years ago (Gehrels et al., 2005; Scott et al., 1995). Many barrier-lagoon systems are able to keep pace with modest rates of RSL rise (Lorenzo-Trueba and Ashton, 2014; McBride et al., 2013), and it is likely that the relative height of the barrier at Robinson Lake to mean sea level has stayed roughly constant during this period, indicating that the sensitivity of our site to marine flooding events has probably remained unchanged over the last millennium.

Robinson Lake (Fig. 1b, c) is separated from the Atlantic Ocean at the southern edge by a natural barrier that was reinforced by a causeway after Hurricane Juan in 2003 (Fig. 1b), and at the northern end by a salt marsh leading into Three Fathom Harbour (Fig. 1c). Tidal mudflats and glacial till exposures are present on the seaward side of the barrier which provide a source for allochthonous sediments. At the northern end of Robinson Lake, the salt marsh is presently ~1 m above mean sea-level and eye-witness accounts (personal communication, John Donahue, 2014) indicate that it was inundated by Hurricane Juan in fall 2003. This indicates that the entry of marine water and sediment into Robinson Lake can potentially occur over the southern barrier and also via the salt marsh to the north. Robinson Lake is shallow (~2 m), with suitable accommodation space for allochthonous sediment input (French, 2006), and a thick layer of submerged aquatic grasses covering its base. The vegetation surrounding Robinson Lake is dominated by dense stands of black spruce (*Picea mariana*). Many of the trees in these stands are dead, also due to the effects (e.g., wind-throw, soil salinization) of Hurricane Juan. Geologically, Robinson Lake is underlain by slate, greywacke and quartzite bedrock (McBride, 1978), but many of the surface features in the region were formed during the most recent glacial period, and include drumlins, moraines, and other glacial depositional landforms (Scott, 1977).

3. Methods

3.1. Field work

The fieldwork, which was undertaken in fall 2014, consisted of coring Robinson Lake using a Livingstone piston corer and a hollow tube fitted with a piston. Two cores were extracted: RL01 (44.651713°, –63.277064°), near the causeway in the center of the lake; and RL02 (44.652148°, –63.277206°), ~40 m further inland (Fig. 1a). Cores were taken at both locations to refusal from a customized platform. The hollow tube and piston were used to collect the water-sediment interface intact while each subsequent drive with the Livingstone piston corer was done approximately 1 m from each other with approximately 30 cm of overlap to ensure continuity. The water-sediment interface cores were extruded vertically near the field site directly into labeled bags at continuous 1 cm intervals. All cores and sediment samples were wrapped in plastic and aluminum foil and placed in split plastic tubes for transportation, and then refrigerated at 4 °C for preservation. Water chemistry, which included salinity, pH, dissolved oxygen, conductivity, total dissolved solids, and temperature, was recorded using a YSI Multiparameter meter at 3 different locations and at different depths to ensure that important limnological variables were characterized throughout Robinson Lake.

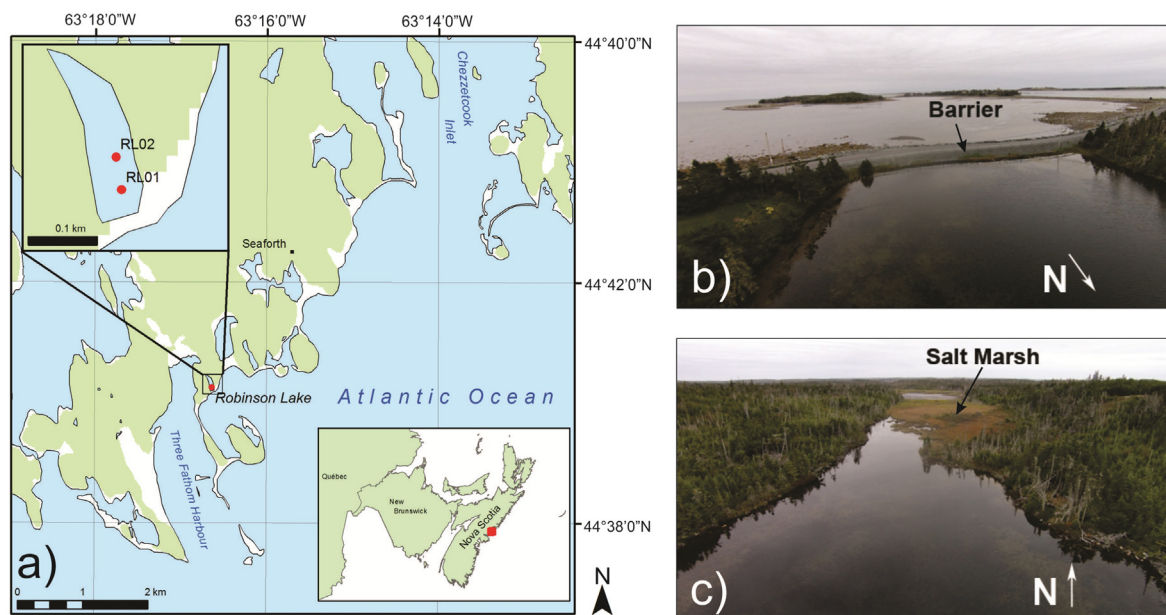


Fig. 1. a) Location of Robinson Lake in the Chezzetcook Inlet, Nova Scotia, Canada. Inset: Location of coring sites RL01 (44.651713°, –63.277064) and RL02 (44.652148, –63.277206) in Robinson Lake. b) Photograph of the Robinson Lake barrier looking south towards the Atlantic Ocean; and c), Photograph looking north towards the salt marsh with the northern tip of Three Fathom Harbour at the very back of the image.

3.2. Laboratory analyses

The sediment cores and extruded upper sediments were subsampled at continuous 1 cm intervals for grain-size analysis using a Microtrac S3500 laser particle size analyzer (lpsa). Pre-treatment of the samples included 30% hydrogen peroxide (H_2O_2) to eliminate organic matter and sodium hexametaphosphate (NaPO_3)₆ to disperse the sediment. Percent organic matter was estimated using loss-on-ignition (LOI; Dean, 1974; Heiri et al., 2001), by burning dried samples at 550 °C and calculating the resulting difference in mass.

Core drives from site RL01 (1000 μm intervals) and RL02 (400 μm intervals) were scanned for elemental composition by XRF using an ITRAX Cox Core scanner at McMaster University's core laboratory (3 kW molybdenum tube set at 30 kV and 25 mA). All drives were also scanned at 400 μm intervals for sediment density by x-radiography. The reporting of individual elements generated through XRF core scanning is usually normalized for “matrix effects”, which include variation in the water, organic matter, and grain size content of the core (Croudace et al., 2006; Weltje et al., 2015). Commonly used normalization parameters include kcps (thousands of counts per second), elements such as Rb, Ti, and Fe, and the Mo inc/Mo Coh ratio (the scattering ratio) (e.g., Chagué-Goff et al., 2016). All individual elemental values were normalized to this latter value (Mo inc/Mo Coh ratio), which has been argued to be a good approximation of sediment core organic matter content which we also demonstrate with our LOI analyses (Chagué-Goff et al., 2016). In addition, several elemental ratios were calculated (Ti/Ca, Fe/Ca, Br/Ti) as these are thought to be reflective of both local- and regional-scale environmental processes occurring at the site (Davies et al., 2015; Gregory et al., 2015; Kylander et al., 2011b). Finally, the sediments from the uppermost samples extruded into bags were not scanned by XRF due to their very high water content and unconsolidated nature but were analyzed for grain-size and LOI and used for the development of the chronology.

3.3. Chronology

The chronology was established using lead-210 (^{210}Pb) and radiocarbon (^{14}C) dating. Lead-210 was used for high-resolution dating of the unconsolidated upper sediments, while radiocarbon dating was

used to establish the older chronological sequence. The ^{210}Pb analyses were performed at the Geotop laboratory in Montréal, Canada, using alpha spectrometry. The ^{210}Pb chronology was built using the constant rate supply (CRS) method, which assumes a varying accumulation rate which is what would be expected at a site with slow lacustrine sedimentation interrupted by episodes of rapid accumulation due to marine intrusions following a TC or major storm (Ghaleb, 2009). Radiocarbon dating was performed at the University of Ottawa's André Lalonde AMS (accelerator mass spectrometry) Laboratory. Terrestrial plant detritus and freshwater shells were used to date the cores and the results were calibrated using the IntCal13 dataset (Reimer et al., 2013). Age-depth models were generated using a Bayesian model in BACON (version 2.2., Blaauw and Christen, 2011).

4. Results

4.1. Core lithology

Core RL01 is 112 cm in length and consists almost entirely of fine-grained mud, with an average grain-size ranging between 12 and 48 μm (Fig. 2a). Prominent peaks in grain size are apparent at depths of 3–4 cm, 37 cm, 51 cm, and 72 cm. Organic matter content is < 25% throughout the core, with the exception of the upper 10 cm which shows a rapid increase (Fig. 2a). Core RL02 is 101 cm long and is silt-rich with an average grain size also ranging from 12 to 48 μm (Fig. 2b). Peaks in mean grain size are also apparent in RL02—occurring in the upper 10 cm of the core, and at 40 cm, 55 cm, 67 cm, and 100 cm, but these are typically less abrupt and of lower magnitude than those in RL01. The organic matter content of RL02 ranges from ~2 to 44% (Fig. 2b) and varies along the core, and increases in the upper 15 cm. Optical images from both cores (Fig. 2) are generally similar, with darker material and a more pronounced stratigraphy near the top of the cores and lighter, more compact sediment, near the center (the upper 5 cm of RL01 and 15 cm of RL02 were not scanned due to the fact that these sediments were extruded into bags). Visually the optical imaging and x-radiography reveals sedimentary structures in both cores. Both cores have darker, finer sediment at the top and base, with a clear transition to greyish, coarser sediments starting at ~35 cm depth in RL01 and ~37 cm depth in RL02, and continuing to deeper levels. The

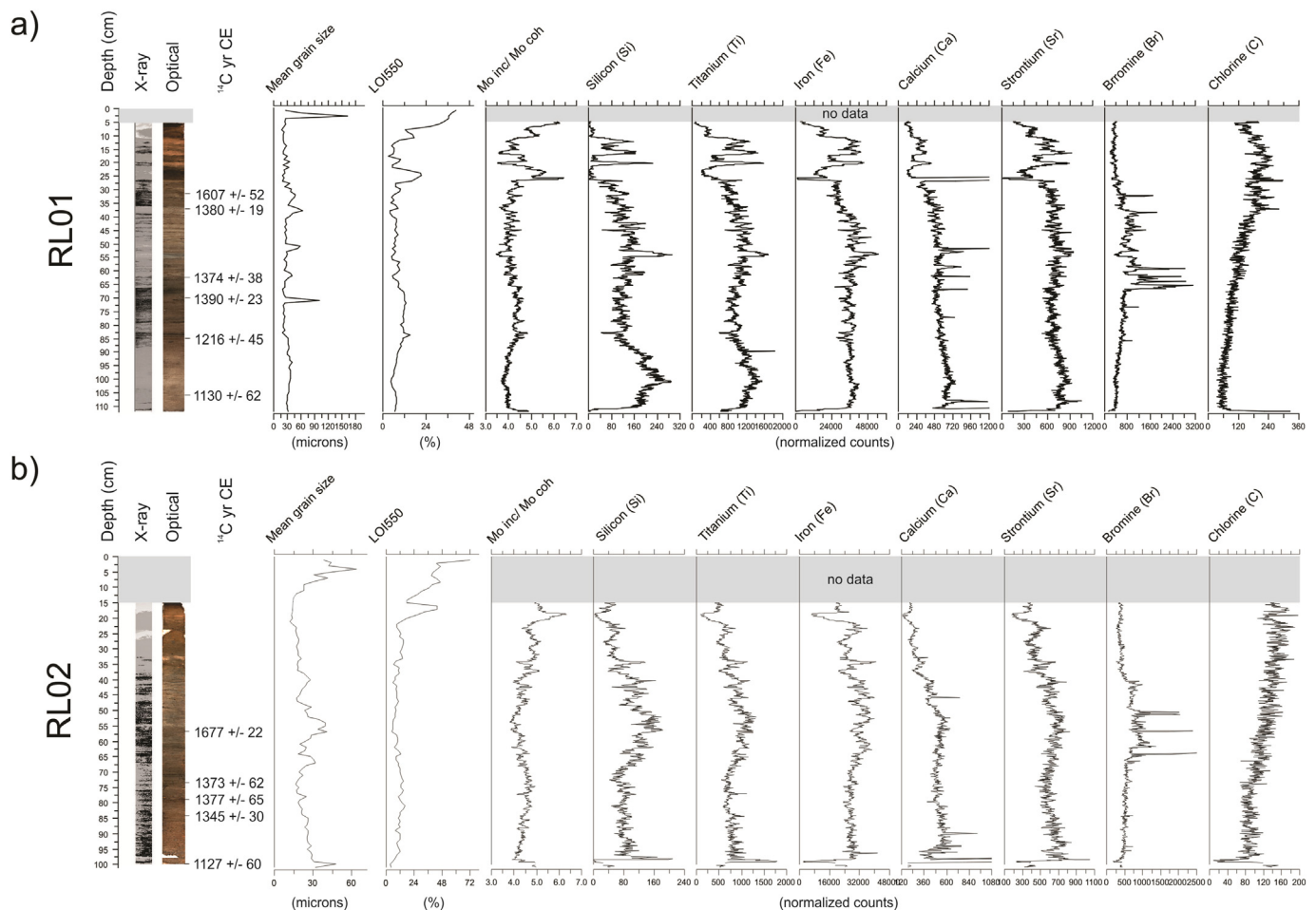


Fig. 2. Plots of X-ray, optical imaging, and uncalibrated ^{14}C dates for cores RL01 (a) and RL02 (b) by depth (cm). The proxy data for both cores includes mean grain-size (μm), organic matter content (%; LOI550), the Mo inc/Mo coh ratio, silicon (Si), titanium (Ti), iron (Fe), calcium (Ca), strontium (Sr), bromine (Br) and chlorine (Cl) based on the XRF core scanning (normalized to Mo inc/Mo coh). The horizontal grey bars indicate that these sections were not analyzed by XRF core scanning.

entire lengths of both cores have fine, well-defined laminations, which is a strong indication that there is little to no vertical mixing. A close visual inspection of both cores showed no evidence of erosional unconformities or abrupt changes in lithology or color indicating depositional hiatuses.

4.2. Chronology

The ^{210}Pb dating results indicate that the upper 13 cm of core RL01 were deposited over the last 150 years, whereas the top 13 cm of RL02 accumulated over the last 100 years (Table 1; Supplemental Fig. 1). On average, the modern accumulation rate of RL01 is 0.09 cm/year, while the accumulation rate of RL02 is 0.13 cm/year.

Age-depth models developed with the combined ^{210}Pb results (Table 1) and ^{14}C results (Table 2) are shown in Fig. 3. One date from core RL02 (Table 2; UOC-2053) was left out of the age-depth model due to probable contamination error, but is plotted in Fig. 3. The accumulation rates vary between the cores, with core RL01 showing an inflection at 25–35 cm depth, and core RL02 showing a more linear trend. In both cases, the age-depth models indicate that sedimentation began at or just after 800 cal yr BP (~ 1150 CE). Thus, the average sediment accumulation rates for both cores are 0.12–0.13 cm/year, which means each 1 cm sample represents between 7 and 8 years of deposition (although this rate varies, especially for the most recent uncompacted sediments).

4.3. XRF elemental composition

As mentioned, all elemental values were normalized using the incoherent-coherent scattering ratio (Mo inc/Mo coh), although the pattern of change did not vary significantly from the primary XRF data or the data normalized to total counts. A visual inspection of the down-core variation in this ratio shows that it is generally correlated with organic matter content (Fig. 2). To quantify the strength of this relationship, all Mo inc/Mo coh values were averaged at the same 1 cm intervals as the LOI data, and the results are plotted in Fig. 4. These plots show that organic matter (determined by LOI550) and Mo inc/Mo coh are positively correlated in both cores, with the fit being stronger for RL01 ($R^2 = 0.756$) compared to RL02 ($R^2 = 0.413$). These results indicate that Mo inc/Mo coh is a good proxy for organic matter content as determined by LOI, consistent with the results of other studies (e.g., Chagué-Goff et al., 2016). Variation in this correlation (for example, some of the outliers in RL02), could be explained by factors such as changes in water content (Chawchai et al., 2016; Boyle et al., 2015). Thus, here, the Mo inc/Mo coh ratio provides an adequate means to normalize the raw XRF data for matrix effects as it corresponds to organic matter content relatively closely.

The XRF results include over 50 elements, but here we focus on: a) the most abundant elements; and b) elements that may be important for TC detection. In RL01 (Fig. 2a), there are important fluctuations with high values of Si, Ti, Fe and Sr, while Cl stays consistently high in the top 25 cm of the core. Bromine (Br) however, does not fluctuate until 32 cm depth. There is a relatively large peak in Si and Ti that occurs at 54.7 cm

Table 1
Pb-210 dating results for cores RL01 and RL02. The “nd” symbols are due to the fact that adding the errors to the measured points will bring the value over the maximum age limit of ^{210}Pb dating. In these cases, the calculated ages should be considered minimum ages.

Lab #	Sample ID	Depth (cm)	^{210}Pb activity (dpm/g)	Error (±)	Density (g/cm ³)	^{210}Pb excess (dpm/g)	CRS model (years before 2014)	Error – (years)	Error + (years)	CRS model (years CE)
8599	RL01-D0 0-1 cm	0.5	18.204	0.763	0.164	15.866	2.0	0.09	0.09	2012
8604	RL01-D0 1-2 cm	1.5	21.402	0.816	0.164	19.064	4.7	0.20	0.20	2009
	RL01-D0 2-3 cm	2.5	23.109	0.983	0.196	20.772	8.4	0.39	0.40	2006
8602	RL01-D0 3-4 cm	3.5	22.219	0.962	0.272	19.881	14.2	0.74	0.76	2000
8603	RL01-D0 4-5 cm	4.5	22.500	0.957	0.244	20.163	20.6	1.19	1.24	1993
8600	RL01-D0 5-6 cm	5.5	23.338	0.953	0.210	21.001	27.7	1.78	1.89	1986
8605	RL01-D0 6-7 cm	6.5	19.292	0.748	0.202	16.955	34.5	2.46	2.66	1980
8606	RL01-D0 7-8 cm	7.5	17.366	0.693	0.262	15.029	44.6	3.75	4.25	1969
8607	RL01-D0 8-9 cm	8.5	15.012	0.643	0.364	12.674	62.9	7.22	9.32	1951
8611	RL01-D0 9-10 cm	9.5	11.012	0.526	0.320	8.674	82.9	13.22	22.82	1931
8612	RL01-D0 10-11 cm	10.5	6.727	0.325	0.438	4.389	111.8	27.10	nd	1902
8613	RL01-D0 11-12 cm	11.5	2.809	0.168	0.825	0.472	123.1	34.28	nd	1891
8614	RL01-D0 12-13 cm	12.5	2.949	0.167	0.815	0.612	148.0	52.95	nd	1866
8615	RL01-D0 13-14 cm	13.5	2.960	0.176	0.687	0.622				
8616	RL01-D0 14-15 cm	14.5	2.521	0.156	0.901					
8617	RL01-D0 15-16 cm	15.5	1.951	0.118	1.045					
8618	RL01-D0 16-17 cm	16.5	2.239	0.147	1.000					
8619	RL01-D0 17-18 cm	17.5	2.349	0.156	0.876					
8620	RL01-D0 18-19 cm	18.5	2.628	0.171	0.648					
8621	RL01-D0 19-20 cm	19.5	3.304	0.187	0.514					
8428	RL02-D0 0-1 cm	0.5	27.646	0.993	0.182	23.886	4.8	0.18	0.19	2009
8429	RL02-D0 1-2 cm	1.5	28.642	1.044	0.071	24.882	6.9	0.28	0.28	2007
8430	RL02-D0 2-3 cm	2.5	24.810	0.900	0.087	21.050	9.4	0.39	0.39	2005
8431	RL02-D0 3-4 cm	3.5	28.311	1.056	0.115	24.551	13.5	0.60	0.62	2001
8432	RL02-D0 4-5 cm	4.5	26.153	0.946	0.117	22.393	17.8	0.85	0.88	1996
8433	RL02-D0 5-6 cm	5.5	23.320	0.862	0.141	19.560	23.1	1.21	1.26	1991
8434	RL02-D0 6-7 cm	6.5	22.939	0.849	0.075	19.179	26.3	1.45	1.52	1988
8435	RL02-D0 7-8 cm	7.5	20.888	0.768	0.134	17.128	32.1	1.96	2.08	1982
8436	RL02-D0 8-9 cm	8.5	21.371	0.781	0.069	17.611	35.7	2.31	2.49	1978
8437	RL02-D0 9-10 cm	9.5	23.017	0.851	0.109	19.257	43.0	3.14	3.49	1971
8438	RL02-D0 10-11 cm	10.5	22.796	0.843	0.089	19.036	50.4	4.18	4.81	1964
8439	RL02-D0 11-12 cm	11.5	21.699	0.799	0.100	17.939	60.6	6.00	7.38	1953
8440	RL02-D0 12-13 cm	12.5	19.980	0.747	0.116	16.220	76.8	9.97	14.53	1937
8441	RL02-D0 13-14 cm	13.5	13.286	0.513	0.162	9.526	101.4	19.39	56.75	1913
8442	RL02-D0 14-15 cm	14.5	8.349	0.317	0.291	4.589				

Table 2

Radiocarbon dates for cores RL01 and RL02 (*was not used in age modelling). The black bar in the plot for the RL02 age-depth model represents the maximum and minimum values of the 2-sigma calibrated age range for this date.

Core	Sample Id	Depth (cm)	¹⁴ C yr BP	Material	Age (2σ calibrated calendar year BP)
RL01	UOC-1065	32	343 ± 52	Organic detritus	500–305
RL01	UOC-2049	38	570 ± 19	Organic detritus	636–594 (56%)
RL01	UOC-1066	61	576 ± 38	Organic detritus	563–535 (39%)
RL01	UOC-2050	71	560 ± 23	Shell	562–527 (50%)
RL01	UOC-1067	84	734 ± 45	Organic detritus	652–527 (50%)
RL01	UOC-1064	106	820 ± 62	Shell	740–563
RL02*	UOC-2053	42	525 ± 20	Organic detritus	901–563
RL02	UOC-2052	57	273 ± 22	Organic detritus	621–611 (4%)
RL02	UOC-1736	73	577 ± 62	Shell	554–513 (92%)
RL02	UOC-1735	79	573 ± 65	Organic detritus	430–358 (50%)
RL02	UOC-2051	85	605 ± 30	Organic detritus	330–287(45%)
RL02	UOC-1734	100	823 ± 60	Organic detritus	660–516
					661–513
					654–544
					907–847(12%)
					832–668(83%)

depth, and also coincides with a decrease in Br and Cl. Another peak in Si is present at 101.5 cm depth, which matches an increase in Ti and an overall decrease in Br. Iron (Fe) also fluctuates but appears to follow a similar pattern to that of Ti and Si. Overall, Br and Cl show different patterns compared to Si, Ti, Fe, Ca, and Sr; Br exhibits very low and stable values from 70 to 110 cm and from 5 to 32 cm, and higher background levels and numerous peaks between 32 and 70 cm. Chlorine (Cl) generally mirrors the organic matter content, and gradually increases towards the top. Increases in mean grain size do not follow those in the elemental data, but generally coincide with the high Br values in the central portion of the core.

In core RL02 (Fig. 2b), the XRF results are similar, showing similar variability between Si, Ti, Fe, and Sr (with higher values in these elements apparent between 38 and 72 cm). Calcium (Ca) and Sr correlate as well, and show generally decreasing values up-core. Bromine (Br) and Cl show patterns that are similar to that of core RL01, with high values of Br between 44 and 66 cm and increasing values of Cl towards the core-top. At a more detailed level, there is one Si peak and one Ti peak that occur at 66.2 cm depth, which also coincide with a dip in Br. Another peak in Si is present at 98.3 cm depth, coincident with an

increase in Ti and Sr, and an overall decrease in Br. As in core RL01, Br generally mirrors the mean grain-size results, with higher values in this element between 40 and 67 cm depth. However, Si and Ti also parallel the grain size results in core RL02, with higher values in the central portion of the core.

Principal Components Analysis (PCA) shows interrelationships between the elemental XRF data and other variables (e.g., mean grain size and LOI) (Fig. 5) (Harff et al., 2011; Rothwell and Croudace, 2015). Biplots of PCA scores for both cores show that elemental variations are generally similar between RL01 and RL02. Strong positive correlations are apparent between Si and Ti, and a strong negative correlation with organic matter content (LOI550), consistent with the visual representation of the stratigraphy (Fig. 2). For core RL01, mean grain size (GS) shows a low correlation with Si, Ti, and organic matter, whereas there is a weak positive relationship between Si, Ti and grain size in RL02. In core RL01, Br is negatively correlated with grain size and somewhat positively correlated with it in RL02. In RL01, Br is not correlated with Si, Ti, or Sr, but varies positively with these elements in RL02. In both cores, Cl shows a weak positive relationship with organic matter and an inverse relationship with grain-size, possibly due to the fact that Cl, as a strong oxidizing agent, has an ability to bind with organic matter (Greenwood and Earnshaw, 1997). The general increasing trend in Cl displayed in both cores (Fig. 2) is likely reflective of increased porosity as sediments become increasingly unconsolidated towards the tops of the cores (e.g., Thomson et al., 2006).

4.4. XRF ratios

A number of elemental ratios were also calculated to better understand the environmental history of Robinson Lake and reconstruct TC activity in the region. Because of the high variability in Br and the similarities in it between cores (Fig. 2), we calculated Br/Ti to estimate the relative contribution of marine versus terrigenous input into Robinson Lake, based on the assumption that high values of Br represent marine incursions caused by TC storm surges and wave activity (Ziegler et al., 2008; Cartapanis et al., 2014), and that Ti is a common indicator of terrestrial detrital material (Haug et al., 2001; Gregory et al., 2015). In addition to Br/Ti, we also used more commonly applied marine and marginal marine elemental ratios, such as Ti/Ca and Fe/Ca, which are often used as indicators of terrestrial input (i.e., precipitation-induced runoff; Gregory et al., 2015). The premise behind the use of these indicators in our study is that they could represent TC-driven precipitation events or long-term climate change by recording sedimentary changes in weathering and precipitation driven runoff into Robinson Lake.

Elemental ratios show similarities between both cores: Ti/Ca and Fe/Ca are highly correlated within both cores (RL01 and RL02), and

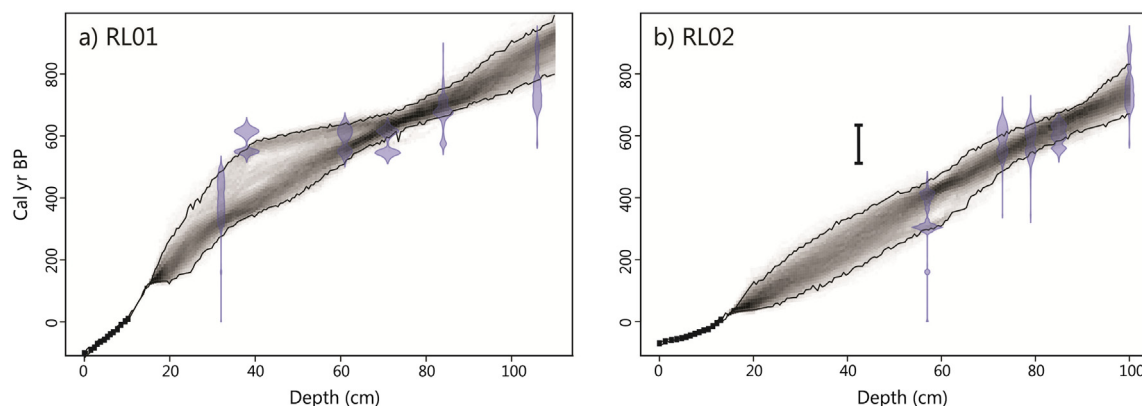


Fig. 3. Age-depth models (based on BACON) for cores RL01 (a) and RL02 (b). The individual ²¹⁰Pb dates are shown by black squares in the lower portion of each age-depth model, and the errors of the dates (Tables 1) are generally within the widths of each square. The vertical black bar in (b) represents the calibrated 2-sigma age range of the date that was left out of the age-depth model for that core.

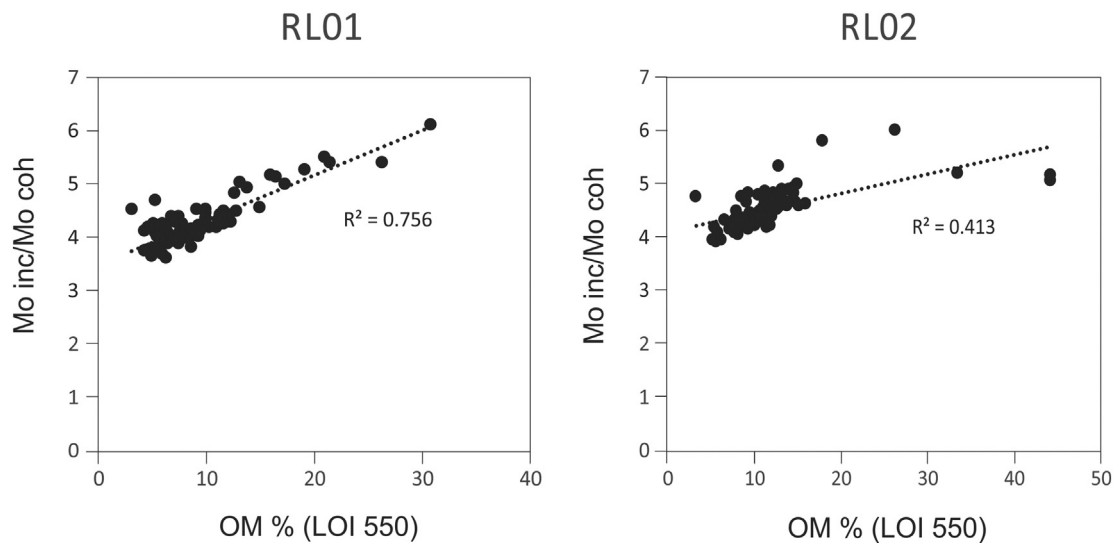


Fig. 4. Scatter-plots of organic matter in percent (LOI550) by Mo inc/Mo coh for cores RL01 and RL02, with linear trend lines and associated coefficient of determination (R^2) values.

show gradually increasing values through time possibly indicative of enhanced runoff in the area from 800 years ago to present. Increases in sediment grain size do not correlate with increases in Ti/Ca or Fe/Ca in either, indicating that sedimentation due to TC-induced precipitation was limited. The one exception is the increase in grain size at ~51 cm in core RL01 that is concurrent with a drop in Ti/Ca and Fe/Ca. The results for Br/Ti are considerably different, however, with large changes between 35 and 72 cm, which correspond to increases in grain size in both RL01 and 02 (see light grey bar, Fig. 6). Several other increases in Br/Ti, notably at 20 cm in core RL02, appear to be related to a decrease in Ti (rather than an increase in Br) and likely reflect increases in the water and/or organic matter content of the cores and therefore are probably unrelated to TC activity. There is very little variation in Br/Ti below 72 cm in the cores.

5. Discussion

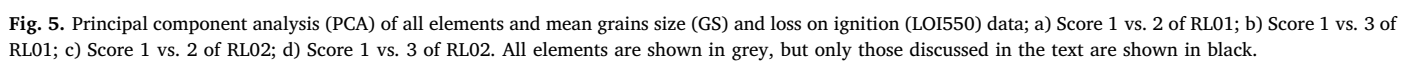
5.1. Tropical cyclone detection and attribution

The grain-size variations in both cores represent fine, “background” sediment overlain by coarser material, likely deposited during episodes of rapid sediment transfer (Toomey et al., 2013). To attribute grain size changes to TC activity, we compared abrupt changes in grain-size in the uppermost part of the cores with a record of the highest storm surges recorded for Halifax, the closest station to Robinson Lake with long-term data, for the period 1919–2008 (ECCC, 2018; Fig. 7a; Table 3). Prominent peaks in grain-size in both RL01 and RL02, when taking into consideration the errors associated with ^{210}Pb dating, center around 2001–2007, and very likely represent overwash-deposited sediment from Hurricane Juan, which struck Robinson Lake on September 29th 2003. The storm surge data recorded for Halifax indicate that Hurricane Juan produced the highest surge height of any tropical cyclone since 1919 for the area (1.6 m). In addition and as previously mentioned, local reports (John Donahue, personal communication, 2014) indicate that no other event in at least a generation caused as much flooding in the region of Robinson Lake as Hurricane Juan did. Indeed, Hurricane Juan was perhaps the most destructive storm event in Nova Scotia for at least the last century, and perhaps even longer (McTaggart-Cowan et al., 2006), and its impact is recorded in the sediments at Robinson Lake.

Other events that cause marine overwash to occur include winter storms (nor'easters) and tsunamis. In the former case, winter storms can result in storm surges that are comparable to, or even exceed those of,

tropical cyclones. For example, an unnamed winter storm that occurred on February 23, 1967, resulted in a storm surge in Halifax that was of similar magnitude to that of Hurricane Juan (Forbes et al., 2009). However, the lack of any sedimentological evidence for overwash in our sedimentary record from the period 1900 CE to 2014 indicates that Robinson Lake is likely insensitive to winter storms. This may be because winter storms are typically associated with winds from the northeast, and a number of studies indicate that winter storm flooding is often more severe on northeast-facing coasts (Fitzgerald et al., 1994; Dickson, 1978), and Robinson Lake is protected from flooding based on its more south-facing orientation. Indeed, paleotempestological research from New England has shown that more south-facing sites are sensitive to TCs, which generally track northward (as Hurricane Juan did; Fig. 7b), but do not record flooding from winter storms, also because of the direction they face (Boldt et al., 2010; Donnelly et al., 2001). One possible exception at Robinson Lake is a small peak in core RL02 that dates to just before 1990, and may be attributed to the “Perfect Storm” of 1991, a mid-latitude storm which absorbed Hurricane Grace and then struck the coast of Nova Scotia in early November of that year (Cardone et al., 1996). Sedimentary evidence for this event has been identified elsewhere in the region (Tuttle et al., 2004), but the lack of any grain size change associated with this event in core RL01 indicates that this small peak in RL02 is more likely to be related to natural variability in background sedimentation or some other process. Finally, tsunamis do occur in the region—the 1929 Grand Banks Tsunami is one such example (Moore et al., 2007; Fine et al., 2005; Tuttle et al., 2004)—but we lack a sedimentary signal for them as well. This lack of evidence, combined with the rarity of tsunamis compared to TCs in the region, indicates that their presence cannot entirely be ruled-out, but that they are unlikely to represent a significant component of the sedimentary signal at Robinson Lake (Moore et al., 2007; Fine et al., 2005).

We therefore argue that Robinson Lake primarily preserves records of TC strikes, and that winter storms have limited visibility within the sediments at the site. Moreover, it is important to note that Robinson Lake does not record all TC events, as surges for at least 9 other TCs (Fig. 7a) generated no sedimentary signal. It is difficult to relate the presence of overwash layers to TC magnitude (Brandon et al., 2014; Woodruff et al., 2008), and the lack of reliable data on the natural barrier height at Robinson Lake (due to the presence of the road built following Hurricane Juan in 2003) makes it difficult to determine what storm surge height would have been necessary to breach the barrier. However, the data in Fig. 7a suggest that storm surge heights of 1 m or



The grain size and Br results are plotted in Fig. 8 as a function of age

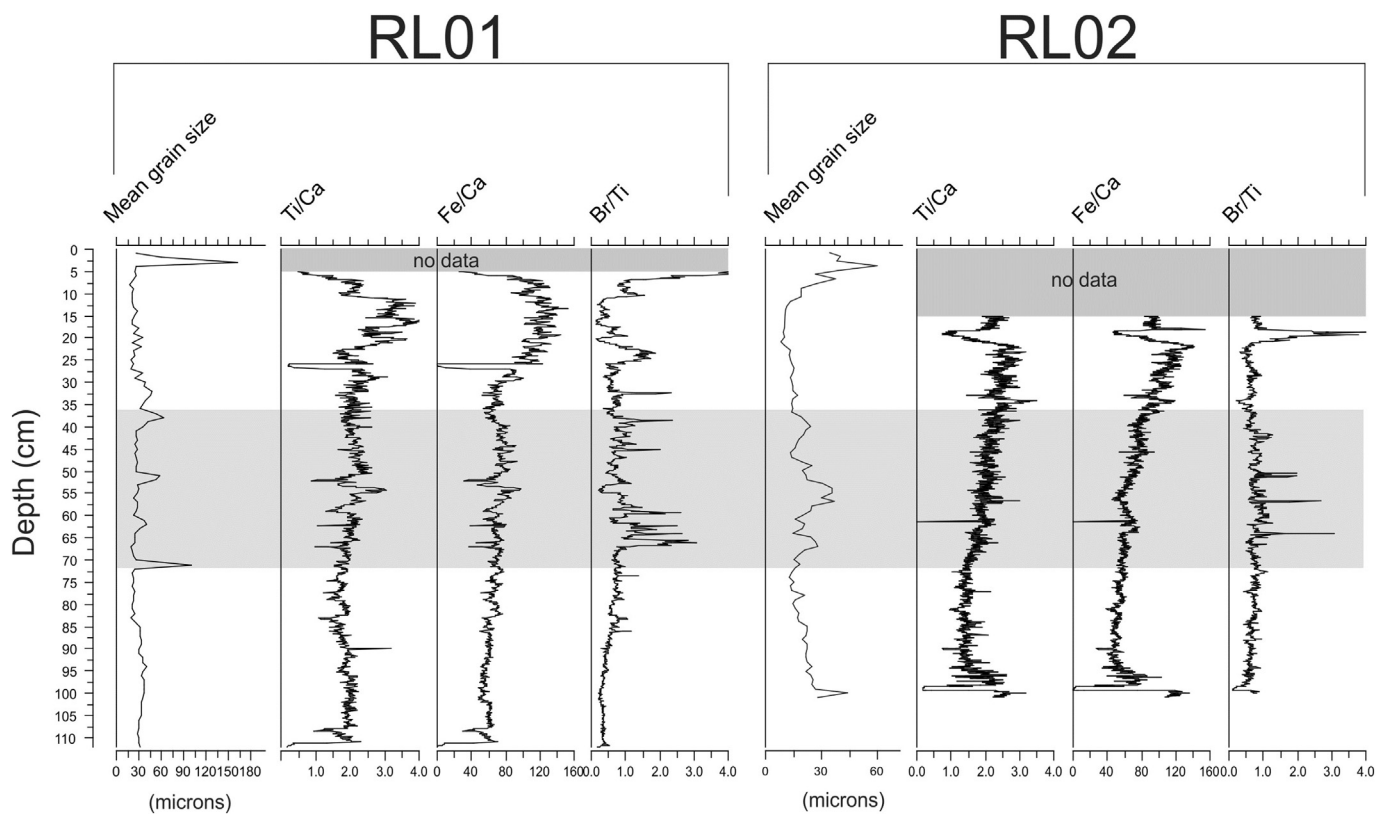


Fig. 6. Plots of mean grain size and elemental ratios (Ti/Ca, Fe/Ca, and Br/Ti) for cores RL01 and RL02, as a function of depth. The dark grey bars at the top show no data for the XRF results. The light grey bar at the center of both cores shows the relationship between grain size peaks and enhanced Br/Ti values.

and show a number of events that very likely represent past TC strikes. In both cores, the increases in grain size are associated with peaks in Br, indicating the overwash of sediment and input of marine organic carbon (MOC) into Robinson Lake. A closer inspection of the data shows an offset in the timing of these events between cores RL01 and RL02, with the RL01 events appearing older. The most likely explanation for this discrepancy is the age-depth model for core RL01 (Fig. 3), which shows two dates (UOC-2047, 570 ± 19 ^{14}C yr BP and UOC-1065, 343 ± 52 ^{14}C yr BP) that, if removed, would generate a near-linear age-depth relationship, similar to that of RL02. Given that these dates were made on bulk organic detritus, the likelihood of a hard-water error that would produce an erroneously old age is high. However, an alternative chronology is also possible; if the omitted date (UOC-2053, 525 ± 20 ^{14}C yr BP) from core RL02 is retained, and the next deepest date (UOC-2052, 273 ± 22 ^{14}C yr BP) is not considered, the age-depth model of RL02 would be similar to that of RL01, with an inflection at around 40 cm depth. This would suggest a high sedimentation rate between ~ 800 to 400 cal yr BP, which is realistic given the degree of sediment overwash inferred for this period. However, as we will show, we argue that the age-depth model in RL02 (Fig. 3) is more reliable due to a close correlation between our data and similar findings from a site in Massachusetts (Donnelly et al., 2015), although we acknowledge that other chronological scenarios are also possible.

The data from both cores at Robinson Lake show evidence of TC strikes at approximately 1475 CE (RL02 2 σ : 1407–1567 CE), 1530 CE (RL02 2 σ : 1501–1661 CE), 1575 CE (RL02 2 σ : 1528–1693 CE), and 1670 CE (RL02 2 σ : 1568–1771 CE) (in addition to the 2003 Hurricane Juan event). Moreover, core RL01, which is closer to the barrier, has much higher average grain-size peaks than RL02, which shows lower-magnitude variations (see x-axis scales for mean grain size in Fig. 8). This difference in grain size is consistent with what would be expected from TC overwash activity, as the coarsest sediment would settle from suspension faster (and hence closer to the barrier) than finer sediments

which would be transported farther into Robinson Lake (Liu and Fearn, 2000; Woodruff et al., 2008). The four events from approximately 1475 to 1670 CE correspond to a period of heightened TC activity inferred from grain size data from Salt Pond, Massachusetts (Donnelly et al., 2015), which occurred from ~ 1400 to 1675 CE (Fig. 8), as well as to data from Thatchpoint Bluehole, Bahamas, which shows heightened TC activity from ~ 1350 to 1650 CE (van Hengstum et al., 2014). Moreover, the most active period at Robinson Lake as per the sedimentary and geochemical data shows evidence for at least three TCs in the 100 years between approximately 1475 to 1575 CE. This frequency (3 events per century) is very similar to the 3.5–4.0 events per century inferred from Salt Pond for roughly the same period of time.

Tropical cyclone intensity is difficult to resolve from sedimentary data, due to the fact that a “small” peak in grain size may represent a TC strike farther away, or with lower wind speed and wave activity, than a lower magnitude event closer to the coring site (Brandon et al., 2014; Woodruff et al., 2008). As mentioned, the modern TC calibration (Fig. 7) suggests that Robinson Lake is recording high magnitude (category 2 or higher) events with surges of at least 1 m, and if the barrier height at Robinson Lake has stayed relatively constant through time, it indicates that the TCs identified in the period from 1475 CE to 1670 were of comparable or greater magnitude. Indeed, at Salt Pond (Fig. 8), Donnelly et al. (2015) indicate that coarse-grained event beds dating from 1300 to 1700 CE point to TCs with intensities greater than any that occurred during historic times. Our data also suggests that during the 1475–1670 CE period in Nova Scotia, TC events were at least of similar magnitude to that of Hurricane Juan.

5.3. Tropical cyclones and climate

The lack of evidence for TC activity from ~ 1150 to 1400 CE in Nova Scotia and Massachusetts suggests that climate conditions were unsuitable for the formation of TCs or that TC tracks at this time were such

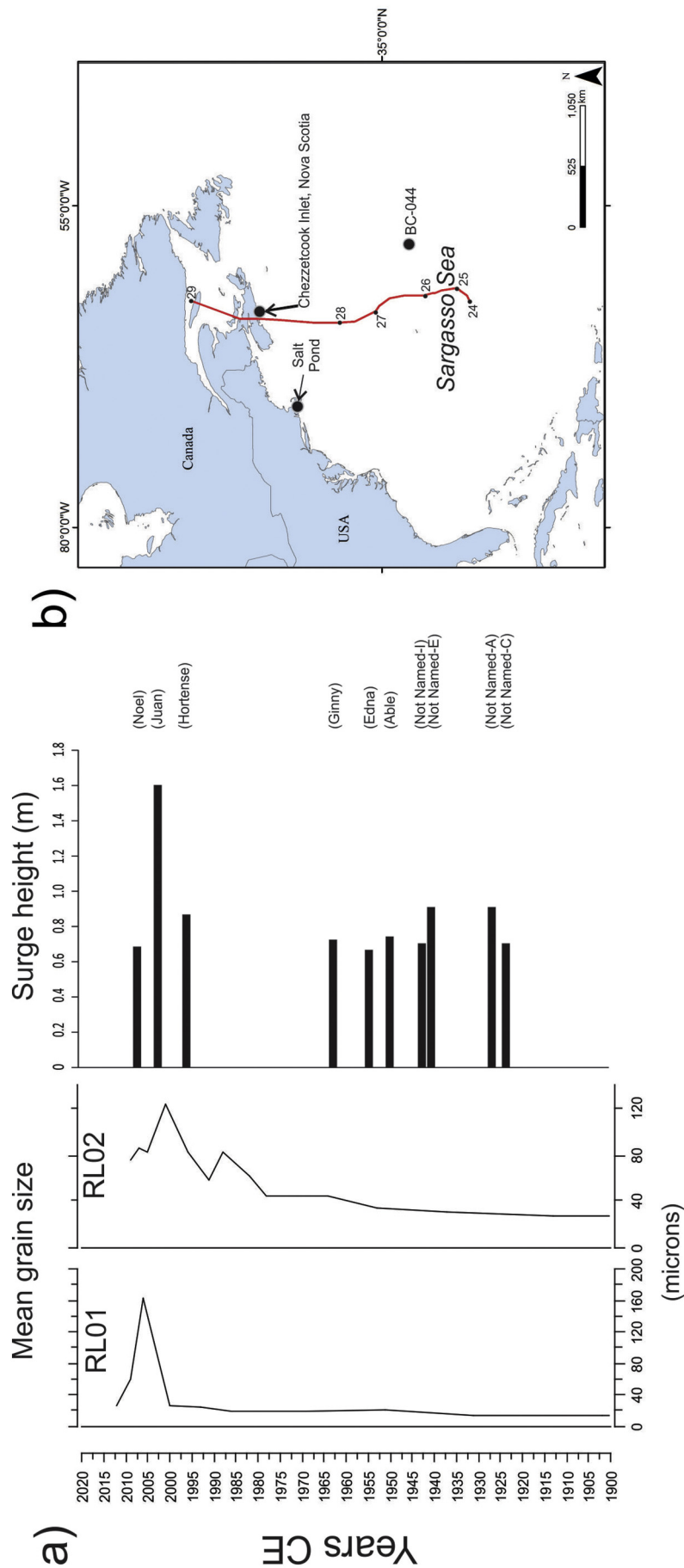


Table 3

Top 10 tropical cyclone surge heights at Halifax, Nova Scotia, for the period from 1919 to 2008 (ECCC, 2018).

Name	Date	Surge height (m)
Juan	September 29, 2003	1.60
Not named-E	September 16, 1940	0.91
Not named-A	August 24, 1927	0.91
Hortense	September 14, 1996	0.87
Able	August 21, 1950	0.75
Ginny	October 29, 1963	0.74
Not named-C	August 26, 1924	0.71
Noel	November 4, 2007	0.71
Not named-I	October 17, 1943	0.70
Edna	September 11, 1954	0.68

that they did not make landfall in this region. Warm sea-surface temperatures (SSTs) are one of the most important factors behind TC formation and trajectory (Tory and Frank, 2010). Relatively cool sea surface temperatures have been noted at this time for this region (Cronin et al., 2010; Keigwin, 1996; Wanamaker et al., 2008; Donnelly et al., 2015), and these may have reduced TC intensity so that few to no events are recorded at these sites. The period from ~1475 to 1675 CE is correlated with an increase in the Atlantic meridional overturning circulation (AMOC) (e.g., Rahmstorf et al., 2015) as well as warmer SSTs inferred from $\delta^{18}\text{O}$ values on planktonic foraminifera from a site in the Sargasso Sea (Fig. 7; Keigwin, 1996). Hurricane Juan passed through the Sargasso Sea (500 km to the west of the core site; Fig. 7b) and rapidly intensified in wind speed as it did so (on September 26–27), before it made landfall near Halifax on September 29. Our data therefore indicates that SSTs in the Sargasso Sea may have had some role at influencing the pre-modern TCs that are recorded at Robinson Lake. Finally, the decrease in TC activity from ~1675 to at least the middle of

the 19th century is closely associated with the Little Ice Age (Fig. 8; Denommée et al., 2014; Keigwin, 1996), which would have brought cooler SSTs to the North Atlantic (Saenger et al., 2009), again decreasing TC intensity at the northern limit of TC tracks (Mann et al., 2009). Despite this, it is important to note that TC activity is controlled by more than just SSTs, with vertical wind shear and other processes being important for their formation, duration, and direction.

5.4. The use of XRF core scanning as a TC indicator

Finally, our work highlights the potential of XRF core scanning as a tool for paleotempestological research. Increasingly, XRF is being used in research on past storm dynamics. For example, Woodruff et al. (2009, 2015), May et al. (2017), and Chagué-Goff et al. (2016) have used different XRF-derived elemental data (such as Br, Fe, Si, Ca, and Sr) to infer or distinguish TC-derived washover deposits. Davies et al. (2015) have suggested that Br (possibly in conjunction with Cl or I) could be a proxy for coastal storm activity, but that its potential needs to be further assessed. While our Br results show a general relationship with sediment grain size, a closer examination of the data shows minor offsets between the two proxies with, in some cases, the grain size peak occurring before the Br peak, and in some cases the grain size peak occurring after (Fig. 8). Some of this discrepancy might be attributable to the different sampling resolution of the grain size data (1 cm) compared to the XRF data (between 400 and 1000 μm). However, a more likely explanation may involve the differential settling of clastic materials and marine organic matter that would generate the larger grain sizes and the Br peaks, respectively. In addition, in the case of Robinson Lake, clastic material and marine water appear to enter the basin over the barrier (as evidenced by the coarser grain sizes in core RL01), but marine water also enters the basin over the salt marsh to the north (as witnessed during Hurricane Juan). Depending on how the elevation of

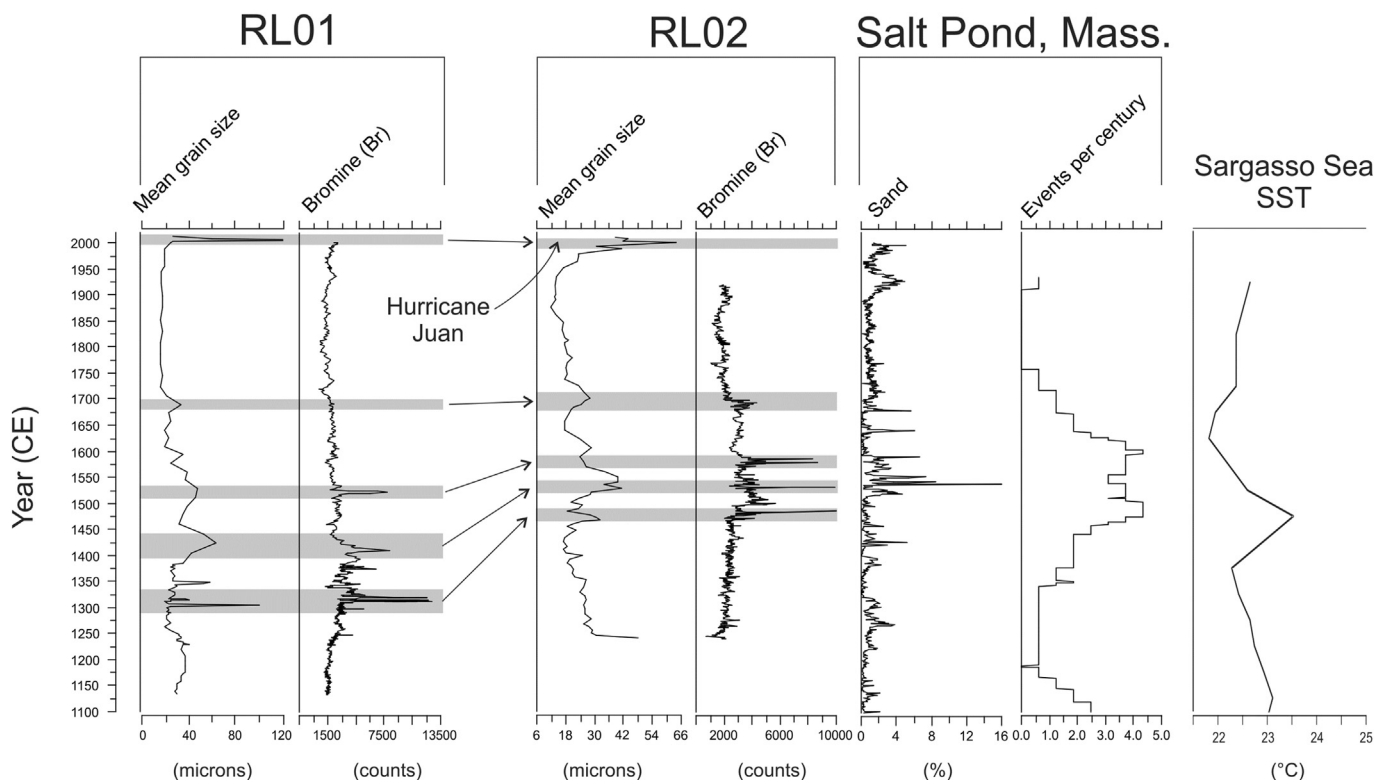


Fig. 8. Mean grain size (μm) and Br (count) plotted by year CE from Robinson Lake. The horizontal grey bars represent likely TC event beds and their correlations between cores RL01 and RL02. Also shown is the Salt Pond, MA, sediment record (% sand) with inferred TC events per century. Finally, the Sargasso Sea SST record, based on the planktonic foraminifer *G. ruber*, is also shown. The SST reconstruction is based on temperature-calibrated $\delta^{18}\text{O}$ data and has been smoothed at 50-year intervals (Keigwin, 1996).

the salt marsh has varied in the past, and variations in barrier height due to TC impacts, the deposition of clastic materials and MOC may not always be synchronous. Clearly, there is potential for using Br as a paleotempestological proxy, but additional work is needed to develop a deeper understanding of its relationship to storm-generated marine incursions.

6. Conclusion

In this paper, we provide the first reconstruction of tropical cyclone activity from the Canadian Maritimes, an understudied region that is important because it helps us understand TC activity at the northern margin of TC tracks, and in so doing may provide important information as to how these events will change under future global warming scenarios (Knutson et al., 2010). Our main finding indicates that on a 800 year timescale, Robinson Lake experienced at least four strikes of high magnitude TCs (i.e., comparable or greater than that of Hurricane Juan) between ~1475 and 1670 CE. These results are consistent with data from Salt Pond, Massachusetts, which shows a similar pattern of TC activity for the last 800 years. While century-scale variability in TC activity can be caused by a number of climate factors, this pattern of changing TC frequency over the last 800 years appears to be related at least in part to sea surface temperatures (SSTs) in the North Atlantic Ocean. We also demonstrate the use of XRF core scanning as a tool for paleotempestological research (e.g., Woodruff et al., 2009; Chagué-Goff et al., 2016), and specifically suggest that sedimentary Br, due to its high abundance in marine organic carbon, is a good complement to more established TC proxy indicators such as sediment grain size.

Our results also provide a basis for future research directions. As mentioned, Robinson Lake appears to be sensitive to TCs and not winter storms, due to the tracks that these respective systems take in relation to the orientation of the coast. However, winter storms (nor'easters) can produce surges and flooding of comparable magnitude to TCs (Forbes et al., 2009), indicating that geological evidence (sedimentary, geochemical, or micropaleontological) is likely available for them. In addition, 2018 saw at least four major storms strike the Canadian Maritimes and New England, and future projections are unclear about how the frequency of these events will change in the coming decades (Wang et al., 2017). It would be very useful to identify sites where winter storms have the potential to be registered in the paleo-record and develop reconstructions to determine the factors that cause long-term variation in these events. In addition, the development of longer paleotempestological records from the Canadian Maritimes (whether for TCs or winter storms) would be advantageous, as it would help contextualize modern-day storm activity and determine whether climate anomalies such as the Medieval Warm Period (Mann et al., 2009) played a role at influencing TC variability. Such information will ultimately be critical for helping us better understand how TC activity in the coming decades will affect eastern Canada.

Data availability

All data is available on Pangaea (www.Pangaea.de).

The following is the supplementary data related to this article.

Acknowledgments

We thank John Donahue for allowing access to Robinson Lake and for sharing valuable personal experiences and Ann Schwartz for accommodation while in the field. Thank you to Marielle Fontaine who provided valuable help in the field. We would also like to thank Shawn Kovacs, Winnie Chan May, and Chelsi McNeill-Jewer from McMaster's School of Geography & Earth Sciences for their help with the analysis. Funding support to Matthew Peros (950-222924) from the Canada Research Chairs program and to Andre Viau (RGPIN/224704-2010), Matthew Peros (RGPIN/405647-2011), and Eduard Reinhardt (RGPIN/

05725-2015) is gratefully acknowledged from NSERC, along with support from the Canada Foundation for Innovation to Eduard Reinhardt and Matthew Peros for laboratory infrastructure and field equipment. Finally, we would like to thank the anonymous reviewers for their constructive feedback.

Appendix A. Supplementary data

Supplementary data to this article can be found online at <https://doi.org/10.1016/j.margeo.2018.09.012>.

References

- Blaauw, M., Christen, J.A., 2011. Flexible paleoclimate age-depth models using an autoregressive gamma process. *Bayesian Anal.* 6, 457–474. <https://doi.org/10.1214/11-BA618>.
- Boldt, K.V., Lane, P., Woodruff, J.D., Donnelly, J.P., 2010. Calibrating a sedimentary record of overwash from Southeastern New England using modeled historic hurricane surges. *Mar. Geol.* 275, 127–139.
- Boyle, J.F., Chiverrell, R.C., Schillereff, D., 2015. Approaches to water content correction and calibration for μ XRF core scanning: comparing x-ray scattering with simple regression of elemental concentrations. In: Croudace, I.W., Rothwell, R.G. (Eds.), *Micro-XRF Studies of Sediment Cores*. Springer Netherlands, Dordrecht, pp. 373–390.
- Brandon, C.M., Woodruff, J.D., Donnelly, J.P., Sullivan, R.M., 2014. How unique was hurricane sandy? sedimentary reconstructions of extreme flooding from New York Harbor. *Sci. Rep.* 4, 7366. <https://doi.org/10.1038/srep07366>.
- Cardone, V.J., Jensen, R.E., Resio, D.T., Swail, V.R., Cox, A.T., 1996. Evaluation of contemporary ocean wave models in rare extreme events: The “Halloween Storm” of October 1991 and the “Storm of the Century” of March 1993. *J. Atmos. Ocean. Technol.* 13, 198–230.
- Cartapanis, O., Tachikawa, K., Romero, O.E., Bard, E., 2014. Persistent millennial-scale link between Greenland climate and northern Pacific Oxygen Minimum Zone under interglacial conditions. *Clim. Past* 10, 405–418. <https://doi.org/10.5194/cp-10-405-2014>.
- Chagué-Goff, C., Hamilton, T.S., Scott, D.B., 2001. Geochemical evidence for the recent changes in a salt marsh, Chezzetcook Inlet, Nova Scotia, Canada. In: *Proceedings of the Nova Scotian Institute of Science*. 41.4, pp. 149–159.
- Chagué-Goff, C., Chan, J.C.H., Goff, J., Gadd, P., 2016. Late Holocene record of environmental changes, cyclones and tsunamis in a coastal lake, Mangaia, Cook Islands. *Island Arc* 25, 333–349.
- Chawchai, S., Kylander, M.E., Chabangborn, A., Löwemark, L., Wohlfarth, B., 2016. Testing commonly used X-ray fluorescence core scanning-based proxies for organic-rich lake sediments and peat. *Boreas* 45 (1), 180–189. <https://doi.org/10.1111/bor.12145>.
- Cronin, T.M., Hayo, K., Thunell, R.C., Dwyer, G.S., Saenger, C., Willard, D.A., 2010. The medieval climate anomaly and little ice age in Chesapeake Bay and the North Atlantic Ocean. *Palaeogeogr. Palaeoclimatol. Palaeoecol.* 297, 299–310. <https://doi.org/10.1016/j.palaeo.2010.08.009>.
- Croudace, I.W., Rindby, A., Rothwell, R.G., 2006. ITRAX: description and evaluation of a new multi-function X-ray core scanner. *Geol. Soc. Lond., Spec. Publ.* 267, 51–63.
- Davies, S.J., Lamb, H.F., Roberts, S.J., 2015. Micro-XRF core scanning in palaeolimnology: recent developments. In: Croudace, I.W., Rothwell, R.G. (Eds.), *Micro-XRF Studies of Sediment Cores*. Springer Netherlands, pp. 189–226.
- Dean, W.E., 1974. Determination of carbonate and organic matter in calcareous sediments and sedimentary rocks by loss on ignition; comparison with other methods. *J. Sediment. Res.* 44, 242–248.
- Denommée, K.C., Bentley, S.J., Droxler, A.W., 2014. Climatic controls on hurricane patterns: a 1200-y near-annual record from Lighthouse Reef, Belize. *Sci. Rep.* 4, 1–7. <https://doi.org/10.1038/srep03876m>.
- Dickson, R.R., 1978. Weather and circulation of February 1978: record or near-record cold east of the continental divide with a major blizzard in the northeast. *Mon. Weather Rev.* 106, 746–751.
- Donnelly, J.P., Woodruff, J.D., 2007. Intense hurricane activity over the past 5,000 years controlled by El Niño and the West African monsoon. *Nature* 447, 465–468. <https://doi.org/10.1038/nature05834>.
- Donnelly, J.P., Bryant, S.S., Butler, J., Dowling, J., Fan, L., Hausmann, N., Newby, P., Shuman, B., Stern, J., Westover, K., Webb, T., 2001. 700 yr sedimentary record of intense hurricane landfalls in southern New England. *Geol. Soc. Am. Bull.* 113, 714–727.
- Donnelly, J.P., Butler, J., Roll, S., Wengren, M., Webb, T., 2004. A backbarrier overwash record of intense storms from Brigantine, New Jersey. *Mar. Geol.* 210, 107–121. <https://doi.org/10.1016/j.margeo.2004.05.005>.
- Donnelly, J.P., Hawkes, A.D., Lane, P., MacDonald, D., Shuman, B.N., Toomey, M.R., van Hengstum, P.J., Woodruff, J.D., 2015. Climate forcing of unprecedented intense-hurricane activity in the last 2000 years. *Earth's Future* 3, 49–65. <https://doi.org/10.1002/2014EF000274>.
- EOCC, 2018. Environment and Climate Change Canada: Oceanographic Data Maps and Statistics. Available from: <https://ec.gc.ca/hurricane/default.asp?lang=En&n=92D2CC35-1> (Accessed multiple times in 2018).
- Emanuel, K., 2003. Tropical cyclones. *Annu. Rev. Earth Planet. Sci.* 31, 75–104. <https://doi.org/10.1146/annurev.earth.31.100901.141259>.
- Fine, I.V., Rabinovich, A.B., Bornhold, B.D., Thomson, R.E., Kulikov, E.A., 2005. The

- Grand Banks landslide-generated tsunami of November 18, 1929: preliminary analysis and numerical modeling. *Mar. Geol.* 215, 45–57. <https://doi.org/10.1016/j.margeo.2004.11.007>.
- Fitzgerald, D.M., van Heteren, S., Montello, T.M., 1994. Shoreline processes and damage resulting from the Halloween Eve Storm of 1991 along the North and South shores of Massachusetts Bay, USA. *J. Coast. Res.* 10, 113–132.
- Forbes, D.L., Manson, G.K., Charles, J., Thompson, K.R., Taylor, R.B., 2009. Halifax harbor extreme water levels in the context of climate change: scenarios for a 1000-year planning horizon. In: Geological Survey of Canada Open File 6346, (22p.).
- Frappier, A.B., Sahagian, D., Carpenter, S.J., González, L.A., Frappier, B.R., 2007. Stalagmite stable isotope record of recent tropical cyclone events. *Geology* 35, 111–114.
- French, J., 2006. Tidal marsh sedimentation and resilience to environmental change: Exploratory modelling of tidal, sea-level and sediment supply forcing in predominantly allochthonous systems. *Mar. Geol.* 235, 119–136. <https://doi.org/10.1016/j.margeo.2006.10.009>.
- Gehrels, W.R., Kirby, J.R., Prokoph, A., Newnham, R.M., Achterberg, E.P., Evans, H., Black, S., Scott, D.B., 2005. Onset of recent rapid sea-level rise in the western Atlantic Ocean. *Quat. Sci. Rev.* 24, 2083–2100. <https://doi.org/10.1016/j.quascirev.2004.11.016>.
- Ghaleb, B., 2009. Overview of the methods for the measurement and interpretation of short-lived radioisotopes and their limits. In: IOP Conference Series: Earth and Environmental Science. 5, pp. 1–13. <https://doi.org/10.1088/1755-1307/5/1/012007>.
- Greenwood, N.N., Earnshaw, A., 1997. *Chemistry of the Elements*, second ed. Butterworth-Heinemann, Oxford.
- Gregory, B.R.B., Peros, M., Reinhardt, E.G., Donnelly, J.P., 2015. Middle-late Holocene Caribbean aridity inferred from foraminifera and elemental data in sediment cores from two Cuban lagoons. *Palaeogeogr. Palaeoclimatol. Palaeoecol.* 426, 229–241. <https://doi.org/10.1016/j.palaeo.2015.02.029>.
- Harff, J., Endler, R., Emelyanov, E., Kotov, S., Leipe, T., Moros, M., Olea, R., Tomczak, M., Witkowski, A., 2011. Late quaternary climate variations reflected in Baltic Sea sediments. In: Harff, J., Björck, S., Hoth, P. (Eds.), *The Baltic Sea Basin*. Springer, Berlin Heidelberg, Berlin, Heidelberg, pp. 99–132.
- Haug, G.H., Hughen, A.K., Sigman, D.M., Peterson, L.C., Rohl, U., 2001. Southward migration of the intertropical convergence zone through the holocene. *Science* 293, 1304–1308.
- Heiri, O., Lotter, A.F., Lemcke, G., 2001. Loss on ignition as a method for estimating organic and carbonate content in sediments: reproducibility and comparability of results. *J. Paleolimnol.* 25, 101–110.
- Itambi, A.C., von Döbenek, T., Mulitza, S., Bickert, T., Heslop, D., 2009. Millennial-scale northwest African droughts related to Heinrich events and Dansgaard-Oeschger cycles: evidence in marine sediments from offshore Senegal. *Paleoceanography* 24, PA1205. <https://doi.org/10.1029/2007PA001570>.
- Keigwin, L.D., 1996. The little ice age and medieval warm period in the Sargasso Sea. *Science* 274, 1504.
- Knutson, T.R., McBride, J.L., Chan, J., Emanuel, K., Holland, C., Landsea, C., Held, I., Kossin, J.P., Srivastava, A.K., Sugi, M., 2010. Tropical cyclones and climate change. *Nat. Geosci.* 3, 157–163.
- Kylander, M.E., Lind, E.M., Wastegård, S., Löwemark, L., 2011a. Recommendations for using XRF core scanning as a tool in tephrochronology. *The Holocene* 22, 371–375. <https://doi.org/10.1177/0959683611423688>.
- Kylander, M.E., Ampel, L., Wohlfarth, B., Veres, D., 2011b. High-resolution X-ray fluorescence core scanning analysis of Les Echets (France) sedimentary sequence: new insights from chemical proxies. *J. Quat. Sci.* 26 (1), 109–117. <https://doi.org/10.1002/jqs.1438>.
- Laidler, R.B., Scott, D.B., 1996. Foraminifera and Arcellacea from Porters Lake, Nova Scotia: modern distribution and paleodistribution. *Can. J. Earth Sci.* 33, 1410–1427.
- Liu, K., 2004. *Paleotempestology*. In: Murnane, R.J., Liu, K.-B. (Eds.), *Hurricanes and Typhoons: Past, Present, and Future*. Columbia University Press, New York, pp. 13–57.
- Liu, K., Fearn, M.L., 2000. Reconstruction of Prehistoric Landfall Frequencies of Catastrophic Hurricanes in Northwestern Florida from Lake Sediment Records. *Quat. Res.* 54, 238–245. <https://doi.org/10.1006/qres.2000.2166>.
- Lorenzo-Trueba, J., Ashton, A.D., 2014. Rollover, drowning, and discontinuous retreat: Distinct modes of barrier response to sea-level rise arising from a simple morphodynamic model. *J. Geophys. Res. Earth Surf.* 119, 779–801. <https://doi.org/10.1002/2013JF002941>.
- Mann, M.E., Woodruff, J.D., Donnelly, J.P., Zhang, Z., 2009. Atlantic hurricanes and climate over the past 1,500 years. *Nature* 460, 880–883. <https://doi.org/10.1038/nature08219>.
- May, S.M., Brill, D., Leopold, M., Callow, J.N., Engel, M., Scheffers, A., Opitz, S., Norpoth, M., Brückner, H., 2017. Chronostratigraphy and geomorphology of washover fans in the Exmouth Gulf (NW Australia) – a record of tropical cyclone activity during the late Holocene. *Quat. Sci. Rev.* 169, 65–84.
- McBride, D., 1978. *Geology of the Ecom Secum area, Halifax and Guysborough Counties, Nova Scotia*. 78 Nova Scotia Department of Mines (20p.).
- McBride, R.A., Anderson, J.B., Buynovich, I.V., Cleary, W.J., Fenster, M.S., Fitzgerald, D., Harris, M.S., Hein, C., Klein, A.H.F., Liu, B., Menezes, J.T., Pejrup, M., Riggs, S.R., Short, A., Stone, G.W., Wallace, D.J., Wang, P., 2013. Morphodynamics of barrier systems: A synthesis. In: Shroder, J., Sherman, J. (Eds.), *Treatise on Geomorphology*. Academic Press, San Diego, pp. 166–244.
- McCloskey, T., Liu, K., 2012. A sedimentary-based history of hurricane strikes on the southern Caribbean coast of Nicaragua. *Quat. Res.* 78, 454–464. <https://doi.org/10.1016/j.yqres.2012.07.003>.
- McTaggart-Cowan, R., Atallah, E.H., Gyakum, J.R., Bosart, L.F., 2006. Hurricane Juan (2003). Part I: a diagnostic and compositing life cycle study. *Mon. Weather Rev.* 134, 1725–1747.
- Miller, D.L., Mora, C.I., Grissino-Mayer, H.D., Mock, C.J., Uhle, M.E., Sharp, Z., 2006. Tree-ring isotope records of tropical cyclone activity. *Proc. Natl. Acad. Sci.* 103, 14294–14297.
- Moore, A.L., McAdoo, B.G., Ruffman, A., 2007. Landward fining from multiple sources in a sand sheet deposited by the 1929 Grand Banks tsunami, Newfoundland. *Sediment. Geol.* 200, 336–346. <https://doi.org/10.1016/j.sedgeo.2007.01.012>.
- NOAA, 2018. National Oceanic and Atmospheric Administration. National Hurricane Center Available from: <http://www.nhc.noaa.gov> (Accessed multiple times from 2014 to 2018).
- Oliva, F., Peros, M., Viau, A., 2017. A review of the spatial distribution of and analytical techniques used in paleotempestological studies in the western North Atlantic Basin. *Prog. Phys. Geogr.* 41, 171–190. <https://doi.org/10.1177/0309133316683899>.
- Rahmstorf, S., Box, J.E., Feulner, G., Mann, M.E., Robinson, A., Rutherford, S., Schaffernicht, E.J., 2015. Exceptional twentieth-century slowdown in Atlantic Ocean overturning circulation. *Nat. Clim. Chang.* 5, 475–480. <https://doi.org/10.1038/nclimate2554>.
- Reimer, P.J., Bard, E., Bayliss, A., Beck, J.W., Blackwell, P.G., Ramsey, C.B., Buck, C.E., Cheng, H., Edwards, R.L., Friedrich, M., et al., 2013. IntCal13 and Marine13 radiocarbon age calibration curves 0–50,000 years cal BP. *Radiocarbon* 55, 1869–1887.
- Rhein, M., Rintoul, S.R., Aoki, S., Campos, E., Chambers, D.P., Feely, R.A., Gulev, S.K., Johnson, G.C., Josey, S.A., Kostianoy, A., Mauritzen, C., Roemmich, D., Talley, L.D., Wang, F., 2013. Observation: ocean. In: Stocker, T.F., Qin, D., Plattner, G.-K., Tignor, M., Allen, S.K., Boschung, J., Nauels, A., Xia, Y., Bex, V., Midgley, P.M. (Eds.), *Climate Change 2013: The Physical Science Basis. Contribution of Working Group I to the Fifth Assessment Report of the Intergovernmental Panel on Climate Change*. Cambridge University Press, Cambridge and New York.
- Rothwell, R.G., Croudace, I.W., 2015. Twenty years of XRF core scanning marine sediments: what do geochemical proxies tell us? In: Croudace, I.W., Rothwell, R.G. (Eds.), *Micro-XRF Studies of Sediment Cores*. Springer Netherlands, Dordrecht, pp. 25–102.
- Saenger, C., Cohen, A.L., Oppo, D.W., Halley, R.B., Carilli, J.E., 2009. Surface-temperature trends and variability in the low-latitude North Atlantic since 1552. *Nat. Geosci.* 2, 492–495. <https://doi.org/10.1038/NGEO552>.
- Schafer, C.T., Medioli, F.S., 2009. Pilot study of fossil evidence of onshore-directed storm events in estuarine sediments: Chezzetcook Inlet, Nova Scotia. *Can. J. Earth Sci.* 46, 193–205.
- Scott, D.B., 1977. *Physiographic and Oceanographic Characteristics of Chezzetcook Inlet, Nova Scotia*.
- Scott, D.B., 1980. Morphological changes in an estuary: a historical and stratigraphic comparison. In: McCann, S.B. (Ed.), *The Coastline of Canada*. Geological Survey of Canada, Ottawa, pp. 199–205. <https://doi.org/10.4095/102212>.
- Scott, D.B., Medioli, F.S., 1980. Living vs. total foraminiferal populations: their relative usefulness in paleoecology. *J. Paleontol.* 814–831.
- Scott, D.B., Brown, K., Collins, E.S., Medioli, F.S., 1995. A new sea-level curve from Nova Scotia: evidence for a rapid acceleration of sea-level rise in the late mid-Holocene. *Can. J. Earth Sci.* 32, 2071–2080.
- Scott, D.B., Collins, E.S., Gayes, P.T., Wright, E., 2003. Records of prehistoric hurricanes on the South Carolina coast based on micropaleontological and sedimentological evidence, with comparison to other Atlantic Coast records. *Geol. Soc. Am. Bull.* 115, 1027–1039.
- Thomson, J., Croudace, I.W., Rothwell, I.G., 2006. A geochemical application of the ITRAX scanner to a sediment core containing eastern Mediterranean sapropel units. *Geol. Soc. Lond., Spec. Publ.* 267, 65–77. <https://doi.org/10.1144/GSL.SP.2006.267.01.05>.
- Toomey, M.R., Curry, W.B., Donnelly, J.P., van Hengstum, P.J., 2013. Reconstructing 7000 years of North Atlantic hurricane variability using deep-sea sediment cores from the western Great Bahama Bank: a 7000 yr record of hurricane activity. *Paleoceanography* 28, 31–41. <https://doi.org/10.1002/palo.20012>.
- Tory, K., Frank, W.M., 2010. Tropical cyclone formation. In: Kepert, J.D., Chan, J.C.L. (Eds.), *Global Perspectives on Tropical Cyclones: From Science to Mitigation*. Vol. 4. World Scientific Series Publishing Co. Pte. Ltd., Singapore, pp. 55–90.
- Tuttle, M., Ruffman, A., Anderson, T., Jetter, H., 2004. Distinguishing tsunami from storm deposits in Eastern North America: the 1929 Grand Banks tsunami versus the 1991 halloween storm. *Seismol. Res. Lett.* 75, 117–131. <https://doi.org/10.1785/gssrl.75.1.117>.
- van Hengstum, P.J., Donnelly, J.P., Toomey, M.R., Albury, N.A., Lane, P., Kakuk, B., 2014. Heightened hurricane activity on the Little Bahama Bank from 1350 to 1650 C.E. *Cont. Shelf Res.* 86, 103–115. <https://doi.org/10.1016/j.csr.2013.04.032>.
- Wallace, D.J., Woodruff, J.D., Anderson, J.B., Donnelly, J.P., 2014. Palaeohurricane reconstructions from sedimentary archives along the Gulf of Mexico, Caribbean Sea and western North Atlantic Ocean margins. In: Martini, I.P., Wanless, H.R. (Eds.), *Sedimentary Coastal Zones from High to Low Latitudes: Similarities and Differences*. Geological Society, London, pp. 481–501. <https://doi.org/10.1144/SP388.12>.
- Wanamaker, A.D., Kreutz, K.J., Schöne, B.R., Pettigrew, N., Borns, H.W., Introne, D.S., Belknap, D., Maasch, K.A., Feindel, S., 2008. Coupled North Atlantic slope water forcing on Gulf of Maine temperatures over the past millennium. *Clim. Dyn.* 31, 183–194. <https://doi.org/10.1007/s00382-007-0344-8>.
- Wang, J., Kim, H.-M., Change, E.K.M., 2017. Changes in northern hemisphere winter storm tracks under the background of Arctic amplification. *J. Clim.* 30, 3705–3724. <https://doi.org/10.1175/JCLI-D-16-0650.1>.
- Weltje, G.J., Bloemsa, M.R., Tjallingii, R., Heslop, D., Röhl, U., Croudace, I.W., 2015. Prediction of geochemical composition from XRF core scanner data: a new multivariate approach including automatic selection of calibration samples and quantification of uncertainties. In: Croudace, I.W., Rothwell, R.G. (Eds.), *Micro-XRF Studies of Sediment Cores*. Springer Netherlands, Dordrecht, pp. 507–534.

- Woodruff, J.D., Donnelly, J.P., Mohrig, D., Geyer, W.R., 2008. Reconstructing relative flooding intensities responsible for hurricane-induced deposits from Laguna Playa Grande, Vieques, Puerto Rico. *Geology* 36, 391–394. <https://doi.org/10.1130/G24731A.1>.
- Woodruff, J.D., Donnelly, J.P., Okusu, A., 2009. Exploring typhoon variability over the mid-to-late holocene: evidence of extreme coastal flooding from Kamikoshiki, Japan. *Quat. Sci. Rev.* 28, 1774–1785. <https://doi.org/10.1016/j.quascirev.2009.02.005>.
- Woodruff, J.D., Kanamaru, K., Kundu, S., Cook, T.L., 2015. Depositional evidence for the Kamikaze typhoons and links to changes in typhoon climatology. *Geology* 43, 91–94. <https://doi.org/10.1130/G36209.1>.
- Ziegler, M., Jilbert, T., de Lange, G.J., Lourens, L.J., Reichert, G.-J., 2008. Bromine counts from XRF scanning as an estimate of the marine organic carbon content of sediment cores: bromine as estimator of sediment composition. *Geochem. Geophys. Geosyst.* 9, 1–6. <https://doi.org/10.1029/2007GC001932>.